Structural phase transformation of nickel nanostructures with synthetic approach conditions

B. C. Behera, A. V. Ravindra, and P. Padhan

Citation: J. Appl. Phys. **115**, 17B510 (2014); doi: 10.1063/1.4864049
View online: http://dx.doi.org/10.1063/1.4864049
View Table of Contents: http://aip.scitation.org/toc/jap/115/17
Published by the American Institute of Physics

Structural phase transformation of nickel nanostructures with synthetic approach conditions

B. C. Behera, A. V. Ravindra, and P. Padhan[a)]
Department of Physics, Indian Institute of Technology Madras, Chennai 600036, India

(Presented 6 November 2013; received 1 October 2013; accepted 4 November 2013; published online 6 February 2014)

Dispersed nanostructures of nickel (Ni) have been synthesized by thermal decomposition of nickel-oleate in the presence of 1-octadecene with controlled synthesis temperature. The evolution of face-centered-cubic (fcc) phase with increasing synthesis temperature from 320 to 365 °C leads to structural phase transformation of nickel nanostructures from hexagonal-close-packed (hcp) to fcc through mixed phases. The saturation magnetization (M_S) of pure fcc and hcp is ~37 and ~0.67 emu/g, respectively. The quenched M_S of hcp Ni nanostructure compared to that of the fcc Ni indicates the presence of frustrated or canted spins in it. As the fcc phase fraction increases the M_S increases, but the observed M_S is significantly larger than the theoretical M_S calculated by considering the contribution solely from the pure hcp and fcc Ni. This enhanced M_S indicates the presence of exchange coupling between the phases and nanoparticles. © *2014 AIP Publishing LLC*. [http://dx.doi.org/10.1063/1.4864049]

Nanostructured materials are of great interest not only for the pursuit of fundamental understanding but also for the wide range of technological applications. The size and morphology of the nanostructures control the optic, electric, magnetic, and catalytic properties.[1–4] Therefore, synthesis process became vital to obtain size and morphology controlled nanostructures. Among various synthesis methods, Park *et al.*[5] reported the high temperature thermal decomposition method, which provides facile and diverse ways to achieve the monodisperse nanocrystals in a large scale using inexpensive and non-toxic metal salts as reactants. Jeon *et al.*[6] synthesized hcp and mixture phases of Ni nanoparticles by reduced nickel ion using reducing agent hydrazine in tetrahydrofuran and oleylamine as capping agent. In contrast to Jeon *et al.*, using polyol process, Chinnasamy *et al.*[7] prepared the pure hcp nickel nanoparticles at higher synthesis temperature in comparison to mixed phase. Nanostructured nickel has attracted much attention because of their numerous practical applications as conducting material, magnetic materials, and catalysts for H_2 generation[8] and growth of carbon nanotubes.[9] There are several reports on the magnetic properties of fcc Ni but the reports on hcp Ni are very rare due to the metastability of the hcp structure. In this article, we report the structural phase transformation of nickel nanostructures with controlled synthesis temperature. In addition, we explore the changes of magnetic properties with the influence of phase fraction of nickel nanoparticles.

For synthesis of Ni nanostructures, 2 g of nickel-oleate complex, 12 ml of 1-octadecene, and 1 ml of oleic acid were properly mixed in five-neck round-bottom flask and stirred by mechanical rotor for 1 h under the flow of N_2 gas. Then, the mixture solution was heated with a constant heating rate of 2 °C/min to the temperature 320 °C (say) and maintained at this temperature for 30 min under the flow of N_2 gas with continuous stirring. The resulting solution was cooled down to room temperature and then ethanol and hexane were added to the solution. Finally, the nickel nanocrystals were separated by centrifugation.

The crystallinity and phases of the products were examined using powder x-ray diffraction (XRD) measurements. The size distribution and morphology of the nanostructures were studied by Field Emission Scanning Electron Microscopy (FESEM). The field dependent magnetization M(H) curves were measured at room temperature using vibrating sample magnetometer (VSM).

Panel (a) of Fig. 1 shows the x-ray spectra of thermolysis products synthesized at temperatures 320, 330, 340, 350, 360, and 365 °C. The x-ray spectrum of the sample synthesized at temperature 320 °C shows pure hcp phase of Ni. However, as the synthesis temperature was increased to 330 °C, the Bragg's peak of fcc phase of Ni appears along with its hcp phase. Both hcp and fcc phases of Ni were observed for the samples synthesized up to temperatures 360 °C. Finally, at temperature 365 °C, the sample revealed only fcc phase of Ni. It should be noted that the high intensity peak (011) of hcp Ni coincides with that of high intensity peak (111) of fcc Ni. So, we have considered well separated (200) and (012) Bragg reflections of fcc and hcp, respectively, to compare the intensity profile of both phases with synthesis temperature, shown in Figs. 1(b) and 1(c). Interestingly, the intensity of (200) peak fcc Ni increases with the increasing synthesis temperature while the intensity of (012) peak hcp Ni decreases. The systematic decrease and increase in the intensity of hcp and fcc phases, respectively, with increasing synthesis temperature is possibly a manifestation of structural change from hcp to fcc. In order to confirm the structural change in Ni nanostructures, we have performed Rietveld structure refinement using GSAS software with EXPGUI.[10] In Fig. 2(a), we have compared the measured and simulated x-ray profiles of the Ni

[a)]Electronic mail: padhan@iitm.ac.in.

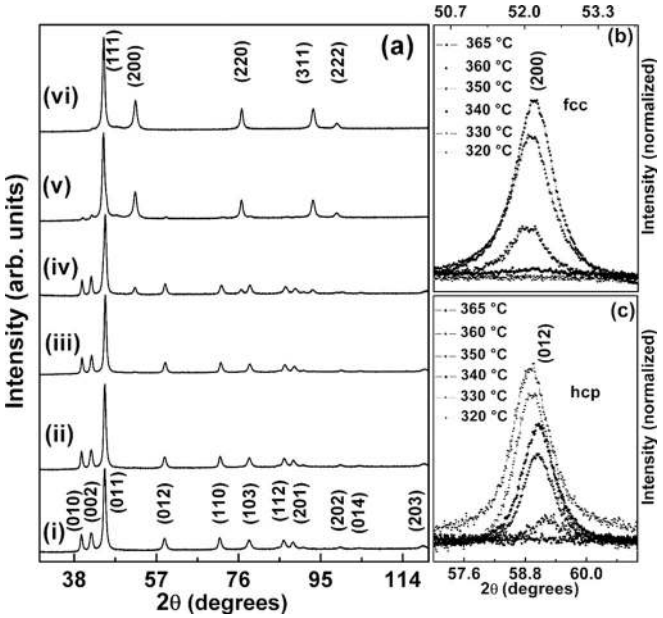

FIG. 1. (a) XRD patterns of nickel nanostructures synthesized at temperatures (i) 320, (ii) 330, (iii) 340, (iv) 350, (v) 360, and (vi) 365 °C, and (b) and (c) show the variation of x-ray intensity of fcc (200) and hcp (012) Bragg's reflections of nickel nanostructures synthesized at different temperatures, respectively.

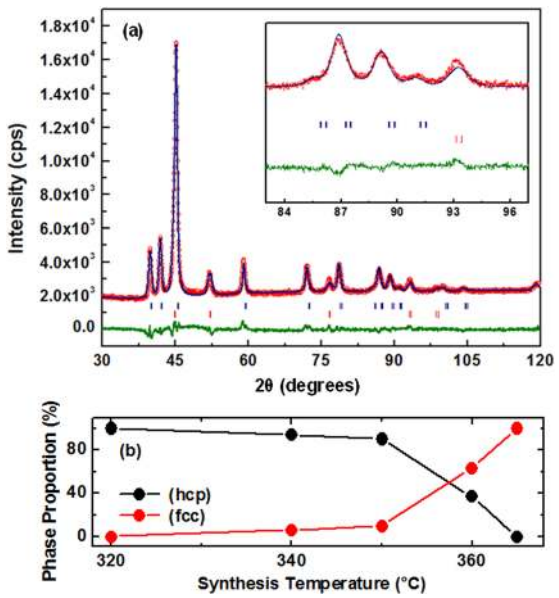

FIG. 2. (a) Measured and simulated (Rietveld method) XRD patterns of nickel nanostructures synthesized at temperature 350 °C and (b) the variation of phase proportion of nickel nanostructures synthesized at different temperatures.

nanostructures synthesized at 350 °C. Clearly, the relative intensity and angular position of the measured x-ray profiles are in good agreement with simulated ones. All the diffraction peaks can be indexed to hcp and/or fcc Ni phase, in good agreement with standard crystallographic data (JCPDS-ICDD Card No. 45–1027 (hcp), 04–0850 (fcc)) and results reported in the literature.[7] However, we have observed that the pure hcp phase of Ni forms at lower synthesis temperature than mixed and pure fcc phases, in contrast to the formation of pure fcc Ni at lower synthesis temperature than the mixed and/or pure fcc phase observed in Ref. 7. The phase proportion yield from the Rietveld refinement of all Ni nanostructures is plotted with the synthesis temperature in Fig. 2(b). The phase proportion of hcp phase varies from 100% to 0% in the synthesis temperature range of 320–365 °C. So, with increasing synthesis temperature, the amount of fcc phase is found to be enhanced and simultaneously the amount of hcp phase is reduced in the same synthesis temperature range. Therefore, it clearly indicates the structural phase transformation of nickel nanostructures from hcp to fcc through mixed phases with increasing synthesis temperature because of the evolution of fcc phase. The lattice parameters, bond lengths, and the average crystallite sizes of Ni nanostructures estimated by Rietveld refinement are listed in Table I. The lattice parameters and bond lengths of these nanostructures do not show any significant variation with the change of synthesis temperature. However, with increasing the synthesis temperature, the average crystallite size of hcp phase decreases while that of the fcc phase increases in the mixed phases nickel nanostructures.

Figure 3 shows the FESEM images of Ni nanostructure synthesized at different temperatures. These images indicate negligible agglomeration of Ni nanostructure. The morphology of the nanostructures looks like nearly spherical. The average particle size calculated by considering 100 particles observed in the FESEM images is significantly higher than the average crystallite size yielded from Rietveld refinement (see Table I). However, we have observed a negligibly small variation of average particle size with increasing synthesis temperature from FESEM images. The negligibly small change in the particle size with varying synthesis temperature from 320 °C to 365 °C indicates that there exist no more precursor for the particles to grow in size after the particles were formed at 320 °C.

The M(H) curves of these nanostructures are shown in Fig. 4. All of these nanostructures show the hysteric field dependent magnetization. The hcp Ni nanoparticles are reported

TABLE I. The calculated lattice parameters, bond lengths, and average particle size of nickel nanoparticles synthesized at different temperatures by Rietveld analysis.

	Lattice parameter (Å)			Bond length (Å)		Average crystallite size (nm)		
Temperature (°C)	hcp		fcc	hcp	fcc	hcp	fcc	FESEM
320	a = 2.643	c = 4.337	…	2.643	…	21	…	29
340	a = 2.637	c = 4.335	a = 3.506	2.637	2.479	28	12	29
350	a = 2.634	c = 4.342	a = 3.531	2.634	2.497	25	18	29
360	a = 2.610	c = 4.318	a = 3.525	2.610	2.493	18	25	30
365	…		a = 3.524	…	2.492	…	22	30

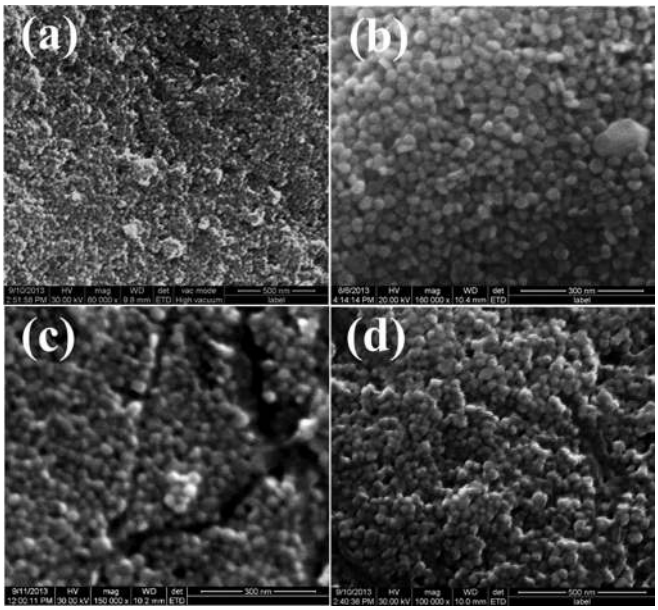

FIG. 3. FESEM images of nickel nanostructures synthesized at temperatures (a) 320, (b) 340, (c) 360, and (d) 365 °C.

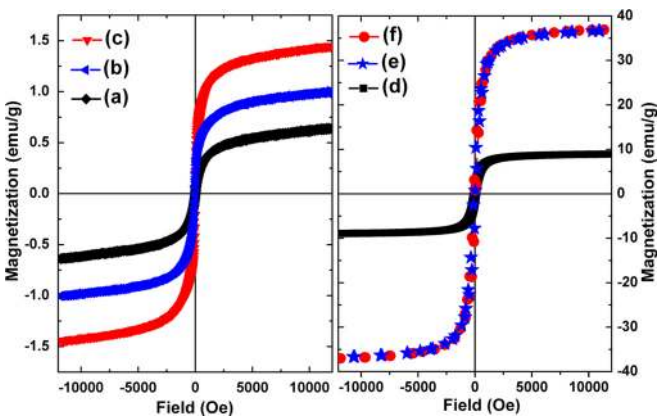

FIG. 4. Field dependent magnetization measured at room temperature of nickel nanostructures synthesized at temperatures (a) 320, (b) 330, (c) 340, (d) 350, (e) 360, and (f) 365 °C.

to be either antiferromagnetic[6] or nonmagnetic[7] or ferromagnetic.[11] We have extracted the saturation magnetization (M_s) by extrapolating the linear part of the hysteresis loop to $\mu_0 H = 0$. The saturation magnetization (M_S) of pure hcp Ni nanostructures (~0.67 emu/g) is quite low compared to that of the fcc phase (~37 emu/g). The quenched M_S of hcp Ni nanostructures compared to that of the fcc Ni indicates the presence of frustrated or canted spins in it. The observed quenched magnetization of hcp Ni is consistent with the reported value of Ni nanoparticles,[11] but the M_S of the fcc Ni is relatively lower than the bulk value (~55 emu/g). The decrease in M_S for fcc Ni nanostructures compared with bulk might be due to the decrease of particle size[12] and the presence of surfactant on magnetic nanoparticles surface.[13,14] The variation of M_S of these Ni nanostructures with synthesis temperature is plotted in Fig. 5. As the synthesis temperature increases from 320 °C, the M_S increases and also the fcc

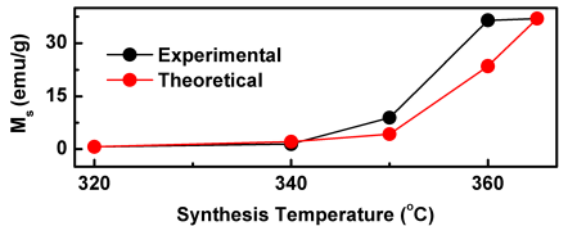

FIG. 5. Saturation magnetization extracted from the room temperature hysteresis loop and calculated theoretically by considering the contribution solely from pure hcp and fcc phases.

phase fraction increases (see Fig. 2(b)). In order to verify the correlation of phase fraction with the M_S, we have calculated the M_S by considering the contribution solely from the pure fcc and hcp Ni. The variation of calculated M_S is also plotted in Fig. 5. As seen in Fig. 5, the experimentally observed M_S is significantly larger than the theoretical M_S. The calculated M_S does not consider any exchange coupling between the fcc and hcp phases which could be the source of relatively higher value of Ms observed in mixed phases nanoparticles.

Ni nanostructures synthesized using thermolysis route exhibit structural phase transformation from hcp to fcc through mixed phases by increasing synthesis temperature from 320 to 365 °C. The quenched M_S of hcp Ni nanostructures compared to that of the fcc Ni indicates the presence of frustrated or canted spins in it. As the fcc phase fraction increases the M_S increases, but the observed M_S is significantly larger than the theoretical M_S calculated by considering the contribution solely from the pure fcc and hcp Ni. This enhanced M_S indicates the presence of exchange coupling between the phases and nanoparticles.

We greatly acknowledge the financial support of New Faculty Seed Grant of IITM.

[1]A. P. Alivisatos, Science **271**, 933 (1996).
[2]R. P. Cowburn, J. Phys. D: Appl. Phys. **33**, R1 (2000).
[3]H. Lee, S. E. Habas, S. Kweskin, D. Butcher, G. A. Somorjai, and P. Yang, Angew. Chem. **118**, 7988 (2006).
[4]C. N. R. Rao, G. U. Kulkarni, P. J. Thomas, and P. P. Edwards, Chem. Eur. J. **8**, 28 (2002).
[5]J. Park, K. An, Y. Hwang, J. Park, H. Noh, J. Kim, J. Park, N. Hwang, and T. Hyeon, Nature Mater. **3**, 891 (2004).
[6]Y. T. Jeon, J. Y. Moon, G. H. Lee, J. Park, and Y. Chang, J. Phys. Chem. B **110**, 1187 (2006).
[7]C. N. Chinnasamy, B. Jeyadevan, K. Shinoda, K. Tohji, A. Narayanasamy, K. Sato, and S. Hisano, J. Appl. Phys. **97**, 10J309 (2005).
[8]Ö. Metin, V. Mazumder, S. Özkar, and S. Sun, J. Am. Chem. Soc. **132**, 1468 (2010).
[9]E. F. Kukovitsky, S. G. L'vov, N. A. Sainov, V. A. Shustov, and L. A. Chernozatonskii, Chem. Phys. Lett. **355**, 497 (2002).
[10]B. H. Toby, J. Appl. Cryst. **34**, 210 (2001).
[11]M. Han, Q. Liu, J. He, Y. Song, Z. Xu, and J. Zhu, Adv. Mater. **19**, 1096 (2007).
[12]E. V. Gopalan, K. A. Malini, G. Santhoshkumar, T. N. Narayanan, P. A. Joy, I. A. Al-Omari, D. S. Kumar, Y. Yoshida, and M. R. Anantharaman, Nanoscale Res. Lett. **5**, 889 (2010).
[13]M. Respaud, J. M. Broto, H. Rakoto, and A. R. Fert, Phys. Rev. B **57**, 2925 (1998).
[14]M. V. Limaye, S. B. Singh, S. K. Date, D. Kothari, V. R. Reddy, A. Gupta, V. Sathe, R. J. Choudhary, and S. K. Kulkarni, J. Phys. Chem. B **113**, 9070 (2009).